Chemistry in Nanodroplets: Studies of Protonation Sites of Substituted Anilines in Water Clusters Using FT-ICR

Sang-Won Lee,† Heather Cox, William A. Goddard, III, and J. L. Beauchamp*

Contribution from the Beckman Institute, California Institute of Technology, Pasadena, California 91125

Received March 20, 2000

Abstract: Water clusters of protonated substituted anilines generated by an electrospray ion source have been investigated using a Fourier Transform ion cyclotron resonance mass spectrometer. It is observed that evaporation kinetics and cluster distributions are highly dependent on sites of protonation in the substituted anilines. Based on the examination of the water cluster distributions of protonated aniline derivatives, the site of protonation is postulated to be the amine group for aniline, *p*-anisidine, *p*-thiomethylaniline, *p*-ethylaniline, and *m*-ethylaniline. The water cluster distributions of these compounds display magic number clusters ($[M + nH_2O]^+$) for $n = 20$, 27, 50, and 52. However, there is no indication of clusters with special stability for *m*-anisidine and *m*-thiomethylaniline, suggesting that these compounds protonate on the ring. DFT calculations have been performed to obtain proton affinities for the different sites of protonation in the substituted anilines and are in good agreement with experimental observation.

Introduction

Solvated ions in the gas phase are frequently referred to as model systems that provide a bridge between the gas-phase chemistry and structure of an isolated ion and its chemistry and structure in solution. This has led to wide-ranging investigations of the solvation of small ions in the gas phase and the effect of solvent on reactivity using various techniques, including high-pressure mass spectrometry,[1] flow tubes,[2] guided ion beam instruments,[3] and Fourier transform ion cyclotron resonance (FT-ICR) mass spectrometry.[4,5] Direct structural information on small solvated ions has been obtained by infrared predissociation spectroscopy[6] and by theoretical ab initio calculations.[7]

Sites of protonation and proton affinities of gas-phase aromatic compounds have attracted considerable interest. Information on the role of solvation in determining the site of protonation has been obtained through the comparison of gas-phase proton affinities with solution-phase basicities. Various aromatic compounds have exhibited linear correlations between gas-phase proton affinity and solution-phase basicity; failure to do so occurs when the site of protonation in the gas phase differs from that in solution.

In the case of substituted anilines, a comparison of the proton affinity of ammonia (853.5 kJ/mol) with that of benzene (750.2 kJ/mol) would suggest that substituted anilines would preferentially protonate on the amine group. However, some substituted anilines, such as *m*-anisidine, *m*-thiomethylaniline, and *m*-ethylaniline, have been observed to protonate on the benzene ring in the gas phase due to the increased electron density (relative to aniline) on the benzene ring.[8] In aqueous solution all of these substituted anilines are amine protonated. Highly localized charge in the protonated amine group of an anilinium ion (**1**) can be more effectively solvated by water molecules than can the extensively delocalized charge of a benzenium ion (**2**). These substituted anilines have different protonation sites

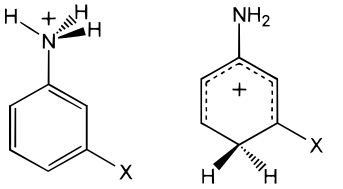

in the gas phase than they do in the solution phase, so it is of interest to determine both their protonation sites in water clusters and the number of water molecules required for proton transfer to occur.

Recently, it has been shown that a carefully optimized electrospray source can be used to produce extensively hydrated molecular ions. The water clusters in this study can contain hundreds of molecules, and so the clusters are nanometer size droplets containing ions of interest. Here we report studies of slow evaporation of the "nanodroplets" containing protonated substituted anilines and their utilization in unambiguous determination of protonation sites in the water cluster. These results

† Current address: Battelle-Pacific Northwest National Laboratories, P.O. Box 999 (K8-98), Richland, WA 99352.

(1) (a) Kebarle, P.; Tang, L. *Anal. Chem.* **1993**, *65*, 972A−986A. (b) Meot-Ner, M.; Speller, C. V. *J. Phys. Chem.* **1986**, *90*, 6616−6624.

(2) (a) Viggiano, A. A.; Dale, F.; Paulson, J. F. *J. Chem. Phys.* **1988**, *88*, 2469−2477. (b) Castleman, A. W., Jr.; Bowen, K. H., Jr. *J. Phys. Chem.* **1996**, *100*, 12911−12944.

(3) (a) Honma, K.; Sunderlin, L. S.; Armentrout, P. B. *Int. J. Mass Spectrom. Ion Processes* **1992**, *117*, 237−259. (b) Armentrout, P. B.; Baer, T. *J. Phys. Chem.* **1996**, *100*, 12866−12877.

(4) Kofel, P.; McMahon, T. B. *Int. J. Mass Spectrom. Ion Processes* **1990**, *98*, 1−24.

(5) (a) Schindler, T.; Berg, C.; Niedner-Schatteburg, G.; Bondybey, V. E. *Chem. Phys. Lett.* **1994**, *229*, 57−64. (b) Schindler, T.; Berg, C.; Niedner-Schatteburg, G.; Bondybey, V. E. *J. Chem. Phys.* **1996**, *104*, 3998−4004.

(6) (a) Yeh, L. I.; Okumura, M.; Myer, J. D.; Price, J. M.; Lee, Y. T. *J. Chem. Phys.* **1989**, *91*, 7319−7330. (b) Cao, Y.; Choi, J.-H.; Haas, B.-M.; Johnson, M. S.; Okumura, M. *J. Chem. Phys.* **1993**, *99*, 9307−9309.

(7) (a) Xantheas, S. S. *J. Phys. Chem.* **1996**, *100*, 9703−9713. (b) Wei, D.; Salahub, D. R. *J. Chem. Phys.* **1997**, *106*, 6086−6094.

(8) Lau, Y. K.; Tse, N. A.; Brown, R. S.; Kebarle, P. *J. Am. Chem. Soc.* **1981**, *103*, 6291−6295.

10.1021/ja0009875 CCC: $19.00
Published on Web 09/08/2000

are used to interpret chemistry observed in water clusters, distinct from the chemistry in both the solution phase and the gas phase.

Experimental Section

All experiments were performed in an external ion source 7T FTICR mass spectrometer that has been described in detail elsewhere.[9] Briefly, the instrument is equipped with a radio frequency-only octopole ion guide, which transfers the ions from the atmospheric pressure ion source into the ICR cell. An electromechanical shutter that is located between the ESI source and the octopole was opened for 2 s to allow ions continuously being generated by the ESI source to enter the octopole ion guide. The radio frequency-field of the octopole was turned on only during this period of time. Argon collision gas (2−5 ms pulse, 10^{-6} Torr) was introduced to moderate the ion kinetic energy while ions were travelling through the octopole ion guide and being trapped in the ICR cell. For production of hydrated substituted anilines a modified version of a commercially available electrospray ion source (Analytica of Branford, Branford, CT) was used that has been described elsewhere.[10] The anilines were dissolved in pure deionized water containing 0.01% acetic acid at concentrations around 100 μM. A syringe pump (Harvard Apparatus, Model PHD 2000, South Natick, MA) injects electrospray solution through a hypodermic stainless steel capillary (63 μm i.d.) at a flow rate of 80−150 nL/min. No nebulizer or counterflowing drying gas was used and the desolvation capillary is operated at room temperature. All substituted anilines were purchased from Aldrich Chemical Co. (Milwaukee, WI) and used without further purification.

DFT calculations have been performed to obtain proton affinities at different sites of protonation of various anilines, including aniline, *m*-/*p*-anisidine, *m*-/*p*-thiomethylaniline, and *m*-/*p*-toluidine.[11] Full geometry optimizations of each compound have been performed at the B3LYP/631G** level with the Jaguar software package[12] running on Origin2000 (Silicon Graphics Inc.). More refined energies for the optimized structures were obtained at the B3LYP/6311G**++ level. Zero-point energy corrections and enthalpy corrections at 298 K were obtained at the B3LYP/6311G** level. It was observed that the DFT calculations (B3LYP/6311G**++//B3LYP/631G**) used in this study overestimate proton affinity of benzene by 4.4 kcal/mol (PA_{calc} = 183.7 kcal/mol, PA_{exp} = 179.3 kcal/mol). The proton affinities for ring protonation of substituted anilines presented here are corrected accordingly.

Results and Discussion

In a previous study from our laboratory,[10] we have shown that water cluster distributions of protonated primary alkylamines display characteristic magic numbers of 20, 27, 50, 52, and 54 (Figure 1a). On the basis of experiments using several amines with different hydrocarbon groups, we proposed structure **3** for the 20-mer water cluster of protonated 1-adamantylamine, where the protonated amine group replaces one of the water molecules in the clathrate structure and an extra neutral water molecule is encapsulated in the cavity. For clusters with fewer than 100 water molecules, solvation is dominated entirely by the protonated amine functional group and not by the hydrophobic hydrocarbon portion of the molecule. We note that it requires three hydrogens from the protonated primary alkylamine to form the proposed structure.

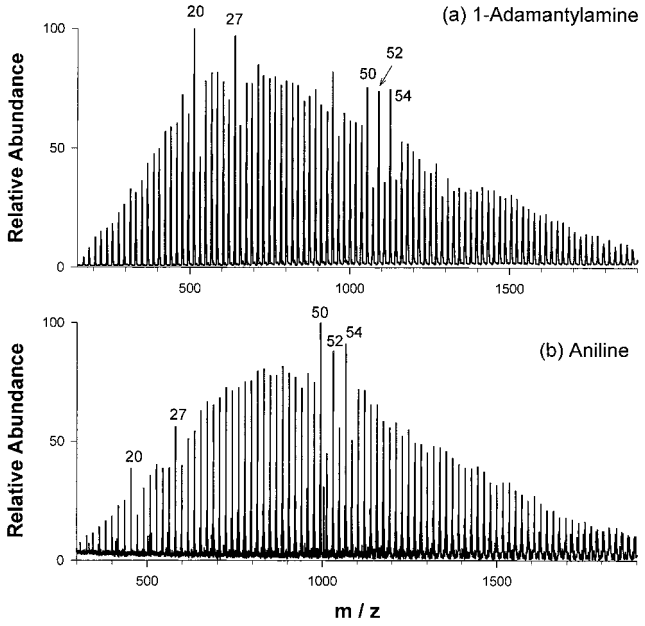

Figure 1. Water clusters of (a) protonated 1-adamantylamine (13 s) and (b) protonated aniline (18 s). Sample concentrations are approximately 100 μM in 0.01% acetic acid solution. Both are amine protonated in water clusters.

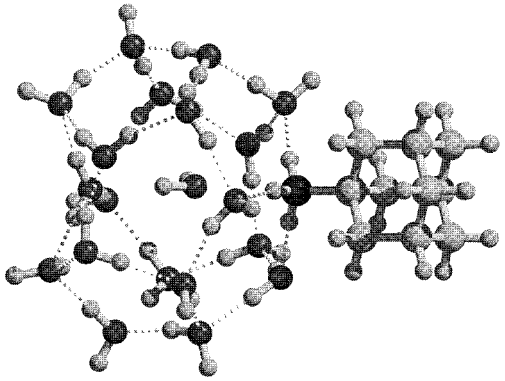

3

A spectrum of solvated protonated aniline is shown in Figure 1b. The question of the preferred site of protonation of substituted aromatics in the gas phase has been the subject of numerous publications.[9,13] Using a combination of STO-3G calculated energy changes for isodesmic proton-transfer reactions and experimentally determined proton affinities of substituted anilines, Hehre, Taft, and co-workers reported that protonation on the aromatic ring of aniline (para position to the amine group, NH_2-benzenium ion, **2**) is only 4−12 kJ/mol less favorable than protonation on the amine nitrogen (anilinium ion, **1**).[14] The water cluster distribution of protonated aniline (Figure 1b) clearly displays magic numbers characteristic of protonated primary alkylamines.

Figure 2 shows the relative intensity ratios of the 20-mer, 27-mer, and 30-mer peaks as a function of time, where the relative intensity ratio is defined as the intensity of the *N*-mer

(9) Rodgers, M. T.; Campbell, S.; Marzluff, E. M.; Beauchamp, J. L. *Int. J. Mass Spectrom. Ion Processes* **1994**, *137*, 121−149.

(10) Lee, S.-W.; Freivogel, P.; Schindler, T.; Beauchamp, J. L. *J. Am. Chem. Soc.* **1998**, *120*, 11758−11765.

(11) To avoid the complication in calculations from the different orientation of the ethyl group in ethylanilines, proton affinities of *m*-/*p*-oluidine were calculated in this study instead of *m*-/*p*-ethylaniline. It is expected that the substituent effects of methyl and ethyl groups are similar. Calculation results from *m*-/*p*-oluidine are accordingly used to explain and compare with experimental results of *m*-/*p*-ethylaniline.

(12) Jaguar 3.5, Schrödinger, Inc.: Portland, OR, 1998.

(13) (a) Freiser, B. S.; Woodin, R. L.; Beauchamp, J. L. *J. Am. Chem. Soc.* **1975**, *97*, 6893−6894. (b) Martinsen, D. P.; Buttrill, S. E. *Org. Mass Spectrom.* **1976**, *11*, 762−772. (c) Dookeran, N. N.; Harrison, A. G. *J. Am. Soc. Mass Spectrom.* **1995**, *6*, 19−26. (d) Chiavarino, B.; Crestoni, M. E.; Rienzo, B. D.; Fornarini, S. *J. Am. Chem. Soc.* **1998**, *120*, 10856−10862.

(14) Pollack, S. K.; Devlin, J. L., III; Summerhays, K. D.; Taft, R. W.; Hehre, W. J. *J. Am. Chem. Soc.* **1977**, *99*, 4583−4584.

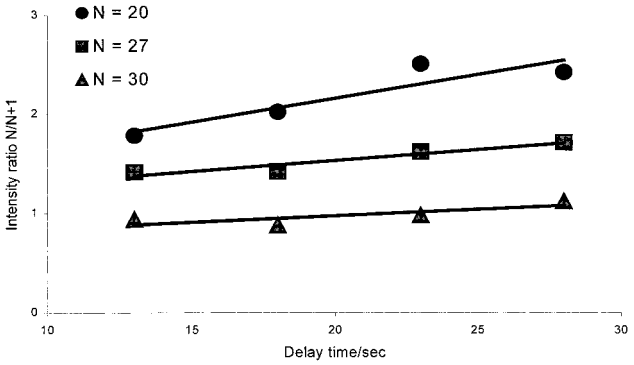

Figure 2. Anilinium ion intensity ratios of three different sets of peaks: 20/21 (circles), 27/28 (squares), and 30/31 (triangles). Intensity ratios are defined as the intensity of the *N*-mer peak over that of the $(N + 1)$-mer peak. The 20-mer and 27-mer are especially stable structures, as indicated by the high-intensity ratio. The 30-mer exhibits no special stability.

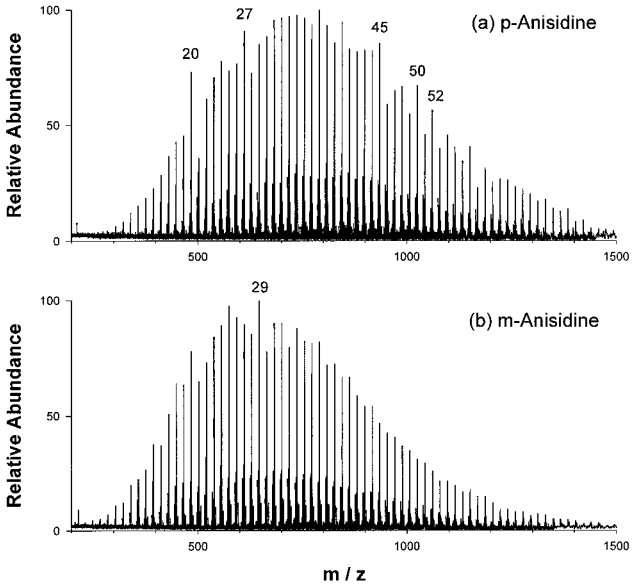

Figure 3. Water clusters of (a) protonated *p*-anisidine and (b) protonated *m*-anisidine detected 23 s after ion accumulation. Sample concentrations are approximately 100 μM in 0.01% acetic acid solution. While *p*-anisidine is observed to be amine protonated, reduction in the intensity of clusters indicative of specific solvation of a protonated amine suggests that protonation occurs on the aromatic ring of *m*-anisidine in water clusters.

peak over the intensity of the $(N + 1)$-mer peak. All clusters show an increase in the relative intensity ratio as a function of time, because the maximum in the distribution of water clusters shifts to lower *m*/*z* values as evaporation proceeds. However, at all times the 20-mer and 27-mer exhibit special stability compared to the 30-mer (and other nonmagic water clusters). This is a strong indication that protonation occurs on the amine group of aniline. The ring-protonated aniline (NH_2-benzenium ion, **2**) does not have a convenient hydrogen bonding site to incorporate into the pentagonal dodecahedron structure of 20-mer water clusters such as shown in structure **3**. It is accordingly expected that ring-protonated aniline would have substantially different cluster distributions from those of primary alkylamines.

Cluster distributions for protonated *p*- and *m*-anisidine ($X = -OCH_3$) are compared in Figure 3. While the cluster distribution of protonated *p*-anisidine exhibits the characteristic magic numbers suggesting amine protonation, protonated *m*-anisidine

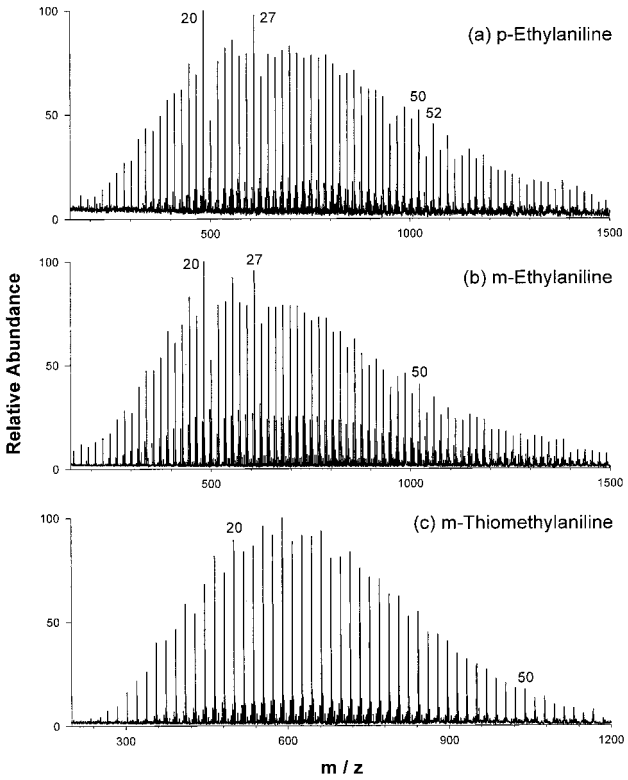

Figure 4. Water clusters of (a) protonated *p*-ethylaniline (18 s), (b) protonated m-ethylaniline (18 s), and (c) protonated *m*-thiomethylaniline (28 s). Sample concentrations are approximately 100 μM in 0.01% acetic acid solution. Both *p*- and *m*-ethylaniline are amine protonated; *m*-thiomethylaniline is ring protonated.

has a markedly different water cluster distribution, showing no specific solvation.[16] This is an indication that protonation occurs on the aromatic ring of *m*-anisidine in water clusters. Clearly, even with a large number of water molecules, the gas-phase behavior of the naked ion is still observed.

Figure 4 shows water cluster distributions observed for protonated *p*-ethylaniline, methylaniline, and *m*-thiomethylaniline.[15] The mass spectrum (Figure 4a) of hydrated *p*-ethylaniline again shows the magic number clusters characteristic of protonated amines, suggesting amine protonation. Interestingly, methylaniline also exhibits the same magic number clusters, indicative of amine protonation (Figure 4b). This indicates a shift in the favored site of protonation to the amine nitrogen from the ring, the preferred site of protonation in the naked ion. The water cluster distribution of protonated *m*-thiomethylaniline (Figure 4c) is quite smooth with no indication of specific solvation. This suggests that protonation occurs on the ring in water clusters.

Density functional calculations have been performed to obtain proton affinities at specific sites on each substituted aniline (Figure 5). The proton affinities obtained with B3LYP/

(15) We were not able to measure water clusters of *p*-thiomethylaniline, since the mass spectrum of *p*-thomethylaniline contains a strong impurity peak, which is not assigned, and overlaps with water cluster peaks of protonated *p*-thiomethylaniline, affecting the relative abundance of cluster peaks.

(16) There is a slight indication of a magic number at $n = 20$ for *m*-anisidine (the average intensity ratio for *m*-anisidine is 1.01 with a standard deviation of 0.15, and the intensity ratio at $n = 20$ is 1.26). However, the intensity ratio at $n = 20$ for *p*-anisidine is 2.02 (average = 1.02, standard deviation = 0.26). It is unclear whether the slight increase in intensity ratio at $n = 20$ for *m*-ansidine is due to a small sub-population of amine-protonated species, a stable isomer at $n = 20$ which does hot resemble the clathrate structures proposed here, or whether it simply occurs as a statistical fluctuation in the data.

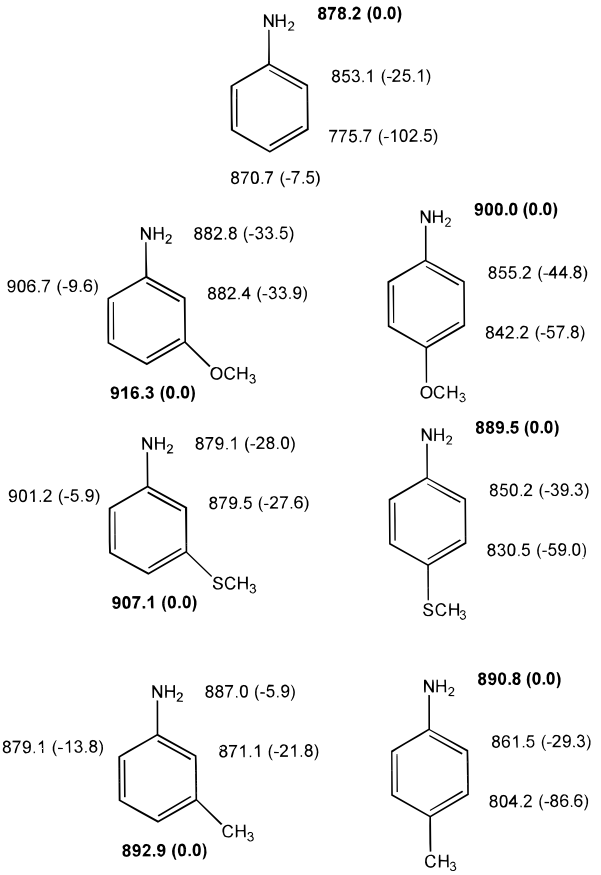

Figure 5. Theoretical site-specific proton affinities (in kJ/mol). Proton affinities were calculated at B3LYP/6311G**++//B3LYP/631G** + ZPE(B3LYP/6311G**). The highest proton affinities are in bold. The proton affinity differences between the specific site of protonation and the site of highest proton affinity are in parentheses. Experimental proton affinities are aniline (882.4), *m*-anisidine (912.9), *p*-anisidine (900.4), *m*-thiomethylaniline (902.1), *p*-thiomethylaniline (N/A), *m*-toluidine (895.8), and *p*-toluidine (896.6).

6311G**++//B3LYP/631G** + ZPE(B3LYP/6311G**) calculations are in good agreement with experimental values. For aniline, ring protonation is calculated to be 7.5 kJ/mol (1.8 kcal/mol) less favorable than amine protonation, which agrees well with the results of Hehr, Taft and co-workers. For all para-substituted anilines used in this study, amine protonation is favored over ring protonation. However, ring protonation is favored over amine protonation for all meta-substituted anilines.

We note that the proton affinity difference ($\Delta PA = PA_{ring} - PA_{amine}$) between the ring protonation and amine protonation for meta-substituted anilines decreases as the substituent's electron donating abilities decrease. For example, the ΔPA's of *m*-anisidine ($X = -OCH_3$) and *m*-thiomethylaniline ($X = -SCH_3$) are 33.5 and 28.0 kJ/mol (8.0 and 6.7 kcal/mol), respectively, while the ΔPA of *m*-toluidine ($X = -CH_3$) is only 5.9 kJ/mol (1.4 kcal/mol). Figure 6 compares the intensity ratios of the 20-mer water clusters of the meta-substituted anilinium ions, plotted against ΔPA. When ring protonation is highly preferred to amine protonation, the 20-mer cluster is not favored. As ΔPA decreases, we observe an increase in intensity ratio, corresponding to increased stability of the 20-mer water cluster and indicating amine protonation.

Kebarle and co-workers measured monohydration equilibria in the gas phase for several substituted anilines.[8] From the measured hydration energy of the first water, they predicted that proton transfer from ring to amino group occurred for

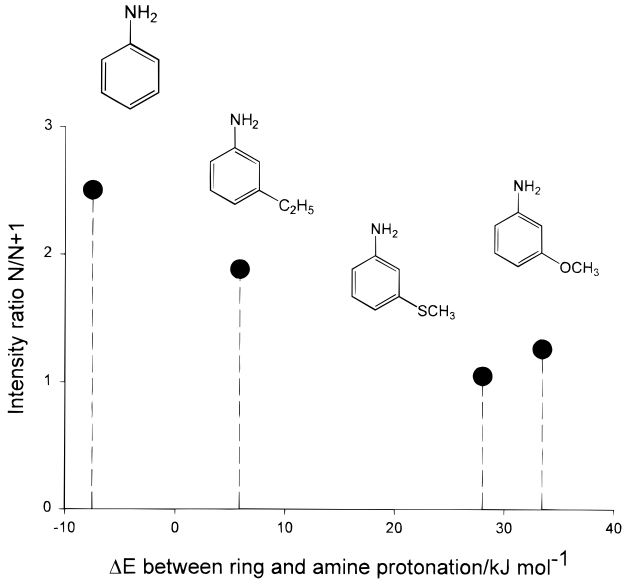

Figure 6. Variation in the ratios of the 20-mer to 21-mer water cluster intensities with the change in proton affinity between ring and amine protonation for aniline, *m*-ethylaniline, *m*-anisidine, and *m*-thiomethylaniline. When ring protonation is highly preferred to amine protonation, the intensity ratio is low. As the difference in energy between the protonation sites decreases, an increase in intensity ratio characteristic of amine protonation is observed.

m-thiomethylaniline, *m*-hydroxyaniline, and methylaniline with one water molecule attached while *m*-anisidine and 1,3-diaminobenzene remained ring protonated. Our results for *m*-ethylaniline indicate that a significant amount of amine protonation occurs with a large number of water molecules. However, contrary to Kebarle's conclusions, we observe a preference for ring protonation in small water clusters of *m*-thiomethylaniline. This difference appears because we calculate the proton affinity difference between ring and amine protonation as 28 kJ/mol, while Kebarle estimated the same difference to be 15 kJ/mol by correlating experimental nitrogen 1s core electron ionization energies with free energies of proton transfer to aniline. We believe that the calculated values are more accurate for species such as *m*-thiomethylaniline, for which the amine protonation and ring protonation differ in energy by less than 50 kJ/mol.

Conclusion

Slow evaporation of water clusters containing 10−100 water molecules ("nanodroplets") of substituted anilines formed by an electrospray ion source has been studied using a FT-ICR mass spectrometer. The generation of hydrated substituted anilines in the gas phase provides a unique possibility for studying the interface between gas phase and solution chemistry in water clusters. Water cluster distributions of substituted anilines are observed to be heavily dependent on their site of protonation in water clusters. While protonated aniline, *p*-anisidine, *p*-ethylaniline, and *m*-ethylaniline exhibit characteristic magic numbers of protonated primary amines, none are observed for *m*-anisidine and *m*-thiomethylaniline. These observations lead to the conclusion that the favored site of protonation in nanodroplets can be readily correlated (as shown in Figure 6) with energetic differences of protonation at different positions in a molecule, as calculated for the unsolvated species. Nanodroplets thus represent a unique environment for studies of solvated ions, since bulk phase behavior is not always observed.

Acknowledgment. The authors are grateful to Dr. Yun Hee Chang for helpful discussions. This work was supported in part by the National Science Foundation under Grant CHE-9727566. Funds for instrument development have been provided by ARPA and the DOD-URI program (ONR-N0014-92-J-1901). H.C. gratefully acknowledges the support of a National Science Foundation graduate research fellowship. We are also indebted to the Beckman Foundation and Institute for the initial funding and continuing support of the research facilities. Computing resources were generously provided by the Material and Process Simulation Center (MSC), also part of the Beckman Institute.

JA0009875